Optical control of nonlinearly dressed states in an individual quantum dot

P.-L. Ardelt, M. Koller, T. Simmet, L. Hanschke, A. Bechtold, A. Regler, J. Wierzbowski, H. Riedl, J. J. Finley, and K. Müller
Walter Schottky Institut and Physik-Department, Technische Universität München, Am Coulombwall 4, 85748 Garching, Germany
(Received 1 March 2016; published 11 April 2016)

We report nonlinear resonance fluorescence of an individual semiconductor quantum dot. By driving a single semiconductor quantum dot via a two-photon transition, we probe the linewidth of two-photon excitation processes and show that, similar to their single-photon counterparts, they are close to being Fourier limited at low temperatures. The evolution of the population of excitonic states with increasing Rabi energy exhibits a clear S-shaped behavior, indicative of the nonlinear response via the two-photon excitation process. Numerical calculations of the nonlinear response using a four-level atomic system representing the manifold of excitonic and biexcitonic states in the quantum dot are in excellent agreement with our experiments and reveal the effect of interactions with LA phonons in the solid-state environment. Finally, we demonstrate the formation of dressed states emerging from a nonlinear two-photon interaction between the quantum dot and the optical excitation field. The nonlinear optical dressing induces a mixing of all four excitonic states that allows direct optical tuning of the polarization selection rules and energies of the dressed states in the artificial atom. We expect our results to play a pivotal role for the generation of nonclassical photon pairs desired for applications in quantum communication and fundamental experiments on quantum optical properties of photons.

DOI: 10.1103/PhysRevB.93.165305

I. INTRODUCTION

The resonant interaction between light and matter lies at the heart of quantum optics [1]. Even the simplest two-level system coherently interacting with an optical field leads to a diverse range of intriguing physical phenomena: the appearance of the Mollow triplet in spectroscopy [2–6], ultracoherent light emission with nonclassical photon statistics [1,7–11], and, most recently, the generation of squeezed states of light [12].

Although the fundamental nonclassical properties of single photons generated by such resonance fluorescence are highly intriguing, for applications in quantum information and communication not only single photons but photon pairs with nonclassical properties are highly desirable [13]. Thus, for over 30 years nonlinear resonance fluorescence, a two- [14] or four-level [15,16] atomic system driven by the simultaneous nonlinear interaction with *two photons*, has been theoretically investigated [14–18]. Nonlinear resonance fluorescence has been predicted to enable a broad range of fundamental quantum optical phenomena from the emergence of nonlinear dressed states [14–18] to two-mode squeezed states [19] and, most importantly for quantum applications, photon bundles with arbitrary quantum statistics [20] and entangled photon pairs [20].

Optically active quantum dots (QDs) have emerged as prototype solid-state systems to probe resonance fluorescence phenomena [4–6,9,12]. Their particular suitability for such experiments results from their large oscillator strength and the two-level nature of their excitonic response [12,21,22]. Resonant driving of excitonic states via one-photon processes has even facilitated single-shot readout of spins [23,24] or phase locking of indistinguishable single photons [8]. While single-photon resonance fluorescence has been extensively studied, nonlinear resonance fluorescence of *two-photon* transitions has been limited to pulsed excitation schemes [25–29] due to the reduced oscillator strength of two-photon transitions. In these investigations intriguing phenomena such as the generation of entangled photons on demand [29] and the reservoir-assisted preparation of excitonic states [27,28,30] have been demonstrated. However, a pulsed optical excitation naturally prevents the formation of an *optically dressed steady state* in the system, the hallmark of resonance fluorescence. To access the theoretically predicted wealth of quantum optical phenomena emerging from nonlinear resonance fluorescence [14–20], the optical control of nonlinearly dressed steady states in a prototypical atomic system remains a fundamental requirement.

In this paper, we report the first direct experimental realization of nonlinear resonance fluorescence on a prototypical four-level system. We directly probe the linewidth of the two-photon transitions of a single optically active QD and demonstrate it to be comparable to that of resonantly driven single-photon transitions. The steady-state population evolution of the exciton and biexciton states exhibits a clear S-shaped behavior indicative of nonlinear light-matter interaction. Notably, the population redistribution in the exciton/biexciton manifold provides evidence for the interaction with LA phonons in the nonlinearly driven system. Finally, we directly observe dressed states in the nonlinearly driven system and demonstrate how the polarization selection rules can be tuned by dressing. We find quantitative agreement with *all* features by numerically calculating the evolution of a nonlinearly driven atomic four-level system coupled to a bosonic reservoir of LA phonons.

II. GENERATION OF HIGHLY COHERENT SINGLE PHOTONS BY RESONANT NONLINEAR EXCITATION

The sample investigated was grown using molecular beam epitaxy. On top of a 14-pair $\lambda/4$ GaAs/AlAs distributed Bragg reflector (DBR) a layer of low-density InGaAs quantum dots is centered in a nominally 260-nm-thick GaAs layer acting as a weak microcavity to enhance the photon extraction efficiency from the surface of the sample [31]. An n-doped layer below the QDs and a Ti/Au metal top contact form a Schottky diode that facilitates control of the electric field which can be used

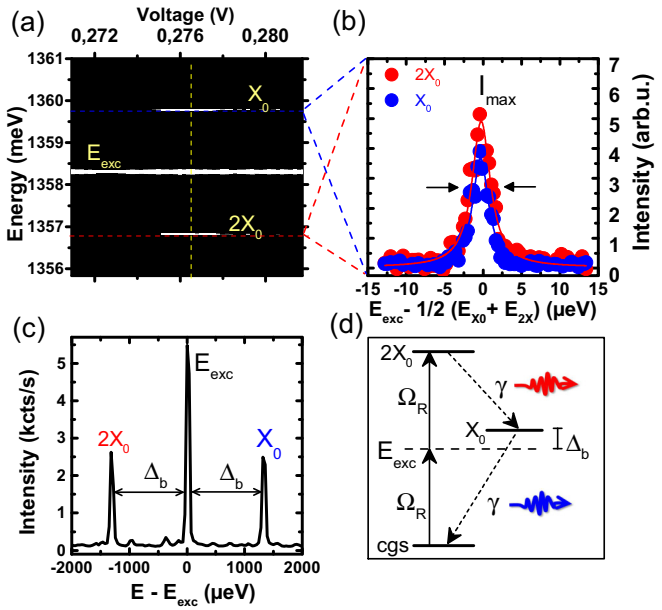

FIG. 1. (a) Voltage-dependent photoluminescence of the neutral exciton X_0 and biexciton $2X_0$ transitions for tuning the excitation laser $E_{\rm exc}$ across the two-photon resonance $cgs \rightarrow\!\!\rightarrow 2X_0$. (b) Detuning-dependent luminescence intensities I_{X_0} and I_{2X_0} to characterize the two-photon transition $cgs \rightarrow\!\!\rightarrow 2X_0$. (c) Emission spectrum for resonant two-photon excitation on resonance. (d) Energy level structure of a QD driven on the two-photon resonance with a Rabi energy Ω_R.

to tune the energies of excitonic transitions of the QD using the dc Stark shift [32].

To characterize the two-photon excitation of individual QDs, we operate the Schottky diode on the neutral charge stability plateau at a lattice temperature of $T = 4.2\,\mathrm{K}$ [27]. The energy-level structure of the QD is presented in Fig. 1(d). While cgs represents the crystal ground state of the system, the first optical excitation corresponds to a charge neutral exciton X_0 (a single excited electron-hole pair e-h), and the second optical excitation corresponds to a charge neutral biexciton $2X_0$ (two e-h pairs). The optically active one-photon transitions from $2X_0 \rightarrow X_0$ and $X_0 \rightarrow cgs$ are detuned by $2\Delta_b$ with respect to each other due to the different attractive Coulomb interactions in the X_0 and $2X_0$ states, respectively [27,32]. This detuning $2\Delta_b$ allows us to directly address the biexciton state $2X_0$ from the cgs via a resonant two-photon excitation process $cgs \rightarrow\!\!\rightarrow 2X_0$ by red detuning the excitation laser from the $X_0 \rightarrow cgs$ transition by half the binding energy $\Delta_b = \frac{1}{2}(E_{X_0} - E_{2X_0})$. Here, the double arrow denotes the two-photon nature of the transition.

Experimentally, we realize this excitation condition by fixing the energy of the excitation laser $E_{\rm exc} = \hbar\omega_L$ close to the two-photon resonance (red detuned from X_0 by $\sim\Delta_b$) and fine-tuning the energy of $2X_0$ relative to the laser using the dc Stark effect [33]. A typical measurement is presented in Fig. 1(a). At a bias of $V = 0.2762\,\mathrm{V}$ applied to the Schottky diode we clearly resolve emission from the $2X_0$ and X_0 transitions in Fig. 1(c), signifying that the two-photon resonance condition has been met. Here, the excitation laser is positioned exactly on resonance at $E_{\rm exc} = \frac{1}{2}(E_{X_0} + E_{2X_0})$. The simultaneous emission of fluorescence results from the cascaded recombination of $2X_0$ via the two *single-photon* transitions $2X_0 \rightarrow X_0 \rightarrow cgs$ [27] indicated in Fig. 1(d). This is a clear signature of resonant two-photon excitation of the biexciton $cgs \rightarrow\!\!\rightarrow 2X_0$ and has been reported previously for QDs subject to pulsed excitation [25–29].

As we drive the two-photon transition $cgs \rightarrow\!\!\rightarrow 2X_0$ using a cw laser with a narrow bandwidth of $\sim$50 neV, measurements of the absorption linewidth of the two-photon transition are facilitated. In Fig. 1(b), we present the integrated intensity of the single-photon transition $2X_0 \rightarrow X_0$ in red ($X_0 \rightarrow cgs$ in blue) as a function of the excitation detuning from the two-photon resonance. The excitation laser detuning is calculated from Fig. 1(a) using the dc Stark effect of the biexciton state $2X_0$ [33]. Thus, the plotted intensities in Fig. 1(b) directly reflect the absorption spectrum of the two-photon transition $cgs \rightarrow\!\!\rightarrow 2X_0$ that displays a clear Lorentzian line shape, as indicated by the fits [solid lines in Fig. 1(b)]. We performed this basic characterization on five different QDs, all of which produced results similar to those presented in Fig. 1(b). For excitation powers of $P_{\rm exc} = 15\,\mu\mathrm{W}$ we obtain linewidths as small as $\Delta\omega_{2X_0\rightarrow X_0} = 2.19\,\mu\mathrm{eV}$ ($\Delta\omega_{X_0\rightarrow cgs} = 2.14\,\mu\mathrm{eV}$) similar to the minimal absorption linewidth of the single-photon transitions of the same QD $\Delta\omega_{cgs\rightarrow X_0} = 1.9\,\mu\mathrm{eV}$. In agreement with the narrow linewidths, Michelson interferometry performed on the emitted photons reveals photonic coherence times up to $T_2(2X_0) = 432\,\mathrm{ps}$ ($T_2(X_0) = 414\,\mathrm{ps}$) at low excitation powers (see Supplemental Material [34]). This indicates near-Fourier-limited coherences within the driven four-level QD system.

III. EVOLUTION OF THE EXCITON AND BIEXCITON POPULATION UNDER TWO-PHOTON EXCITATION

To develop a physical understanding we model the QD as a four-level system consisting of the states $|cgs\rangle$, $|X_0(V)\rangle$, $|X_0(H)\rangle$, and $|2X_0\rangle$ driven by a semiclassical electromagnetic field with Rabi energy Ω_R. Modeling was performed using the Quantum Toolbox in PYTHON [35,36]. Here, the single-exciton state X_0 in Fig. 1(d) is replaced by the two states $X_0(V)$ and $X_0(H)$ that result from the anisotropic e-h exchange interaction and are split by δ_0. We consider the excitation field to be on resonance with the two-photon transition $\hbar\omega_L = \frac{1}{2}(E_{X_0} + E_{2X_0})$, change into a frame rotating with the laser frequency ω_L, and use the rotating-wave approximation. The Hamiltonian in matrix form $H_{ij} = \langle j|\hat{H}|i\rangle$ in the bare-state basis $i, j = cgs, X_0(V), X_0(H), 2X_0$ then reads:

$$H_{\rm total} = H_0 + H_{\rm int} = \begin{pmatrix} 0 & -\frac{\Omega_V}{2} & -\frac{\Omega_H}{2} & 0 \\ -\frac{\Omega_V}{2} & \Delta_b - \frac{\delta_0}{2} & 0 & -\frac{\Omega_V}{2} \\ -\frac{\Omega_H}{2} & 0 & \Delta_b + \frac{\delta_0}{2} & -\frac{\Omega_H}{2} \\ 0 & -\frac{\Omega_V}{2} & -\frac{\Omega_H}{2} & 0 \end{pmatrix}$$

Note that we assign similar Rabi energies $\Omega_{H(V)} = \Omega_R$ to both single-photon transitions corresponding to a diagonally polarized excitation field $|D\rangle = \frac{1}{\sqrt{2}}(|H\rangle + |V\rangle)$ as present in our cross-polarized resonance fluorescence setup. We only allow the optically active transitions $cgs \rightarrow X_0$ and $X_0 \rightarrow$

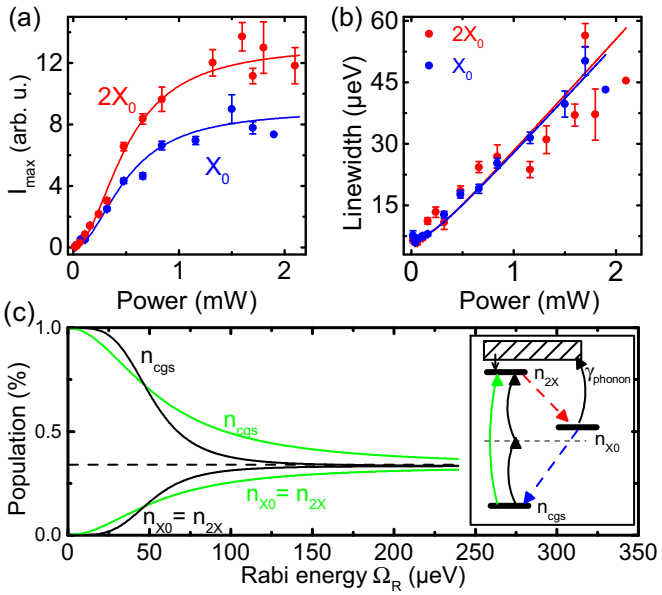

FIG. 2. (a) S-shaped power dependence of the maximum intensities $I_{\max}$ with theoretically calculated intensities from the population distribution n_i including LA-phonon coupling [schematically presented in the inset in (c)]. (b) Linewidth of the two-photon transition as a function of the excitation power. (c) Calculated evolution of the populations n_i under resonant two-photon excitation (black) and single-photon excitation (green) *without* LA-phonon coupling. The excitation processes are illustrated in the inset. Agreement with the recorded populations in (a) is only established by including the coupling to LA-phonons with the rate γ_{phonon}.

$2X$ and include the spontaneous emission between $2X \rightarrow X_0(H/V)$ and $X_0(H/V) \rightarrow cgs$ as collapse operators with rates γ_i, as illustrated in Figs. 1(d) and 3(a) (see Supplemental Material for details).

The excitation laser couples $|cgs\rangle$ and $|2X_0\rangle$ via two-photon excitation. Thus, for the steady-state solution of the system ρ_{ss}, the coupling $cgs \rightarrow\rightarrow 2X_0$ leads to a redistribution of the populations $n_i = Tr(\rho_{ss}|i\rangle\langle i|)$ between the four states $i = cgs, X_0(V), X_0(H), 2X_0$. In Fig. 2(a), we present the maximum intensities $I_{\max}$ of the two-photon absorption spectra [similar to Fig. 1(b)] as a function of increasing excitation power P_{exc} for both transitions $2X_0 \rightarrow X_0$ and $X_0 \rightarrow cgs$. The relative intensities $I_{\max}$ are directly proportional to the populations of the upper state. Thus, the biexciton population is proportional to $I_{\max}(2X_0) \propto n_{2X_0}$. The exciton population is proportional to the sum of the populations $I_{\max}(X_0) \propto (n_{X_0(V)} + n_{X_0(H)})$ since we do not resolve the fine-structure splitting δ_0 between $X_0(V)$ and $X_0(H)$ with the limited resolution of the grating spectrometer used in these experiments.

We clearly resolve two features in Fig. 2(a): first, an S-shaped power dependence of the population evolution and, second, an increased population redistribution into $2X_0$ compared to X_0 for increasing P_{exc}. The S shape is qualitatively understood by considering the nonlinear nature of the excitation process: For a resonantly driven two-photon transition, its Rabi energy depends on the square of the single-photon Rabi energy Ω_R with $\Omega \propto \frac{\Omega_R^2}{\Delta}$ [37] and induces an additional curvature in the power-dependent saturation of the populations n_i. We present the numerically calculated evolution of the steady-state populations n_i for the states cgs, X_0, and $2X_0$ in Fig. 2(c). All populations n_i saturate against a relative value of $1/3$ with increasing Ω_R. For comparison, the green curve in Fig. 2(c) shows the evolution of the populations n_i for the same system excited via a single-photon transition from a semiclassical light field in resonance with the $cgs \rightarrow 2X_0$ transition. We clearly observe that the saturation behavior of the populations n_i towards $1/3$ remains; however, the S shape of the power dependency is flattened.

While the shape of the population evolution is well reproduced by the model, the increasing distribution of population into the biexciton state $n_{2X_0} > n_{X_0}$, observed in Fig. 2(a), is not. In order to model the redistribution we extend the Hamiltonian $H_{QD} + H_{\text{int}}$ by including coupling to the longitudinal-acoustic (LA) phonon bath in the GaAs environment:

$$H_{QD-\text{phonon}} = \sum_i |i\rangle\langle i| \sum_q \lambda_q^i (\hat{b_q}^\dagger + \hat{b_q}), \qquad (1)$$

where $\hat{b_q}^\dagger$ ($\hat{b_q}$) describes the creation (annihilation) operator of an LA phonon with a wave vector q and energy $\hbar\omega_q$. The detuning-dependent coupling strength between the charge carrier states $i = X_0(V), X_0(H), 2X_0$ and the LA-phonon reservoir is described by λ_q^i. Most importantly, the resulting charge-carrier-phonon-interaction spectrum $J(\Delta\omega)$ is highly sensitive to the energy detuning of the excitation laser $\hbar\omega_L$. Only for positive detunings $\Delta\omega_{i\rightarrow j} = \omega_L - \omega_{i\rightarrow j} > 0$ of the excitation laser with respect to the optical transition $i \rightarrow j$ does the spectrum acquire considerable values since LA phonons are frozen out at low temperatures and phonon emission processes dominate [28,30,38,39]. When the excitation laser resonantly drives $cgs \rightarrow\rightarrow 2X_0$, it is blue detuned from $2X_0 \rightarrow X_0$ ($\Delta\omega_{2X_0\rightarrow X_0} = +\Delta_b > 0$) and red detuned from $X_0 \rightarrow cgs$ ($\Delta\omega_{2X_0\rightarrow X_0} = -\Delta_b < 0$). Thus, although we include both interactions in the Hamiltonian $H_{QD-\text{phonon}}$, it influences only the population redistribution between X_0 and $2X_0$.

For a blue detuning of the excitation laser of $\Delta\omega_{2X_0\rightarrow X_0} = \Delta_b = +0.93$ meV, the charge-carrier-LA-phonon interaction will lead to an incoherent population transfer from X_0 to $2X_0$ via a phonon-assisted excitation process [38] [inset in Fig. 2(c)]: It works effectively as an incoherent population pump rate γ_{phonon} from X_0 to $2X_0$. This pump rate γ_{phonon} increases the steady-state population of the biexciton n_{2X_0} with respect to the exciton n_{X_0}. To calculate the resulting population redistribution, we transform the Hamiltonian $H = H_{QD} + H_{\text{int}} + H_{QD-\text{phonon}}$ into the polaron frame (see Supplemental Material for details) [40]. The resulting relative populations are fit to the intensities of the single-photon transitions $I_{2X_0\rightarrow X_0} \propto n_{2X_0}$ and $I_{X_0\rightarrow cgs} \propto n_{X_0}$ in Fig. 2(a) by varying the dipole moment of the two-photon transition. We achieve excellent agreement between the calculated populations n_{2X_0} and n_{X_0} and the recorded intensities by including the charge-carrier-LA-phonon interaction.

From the saturating behavior of the emission intensity with increasing Ω_R, we expect the linewidth of the two-photon transition $\Delta\omega_{cgs\rightarrow\rightarrow 2X}$ to exhibit power broadening. Indeed, plotting the linewidth of the two-photon absorption spectrum

extracted from Fig. 1(b) with a guide to the eye for various P_{exc}, we observe a clear increase of the linewidth $\Delta\omega_{cgs\rightarrow\rightarrow 2X_0}$ with increasing Rabi energy Ω_R. However, although the linewidth broadening qualitatively follows the expected increase of a two-photon power broadening, we emphasize that this is not the only source contributing to a power-dependent linewidth increase. For increasing P_{exc} photon-mediated charging events in proximal defects may lead to charge noise in the QD environment [41,42]. Furthermore, the increased coupling efficiency to LA phonons induces additional dephasing in the system (see Supplemental Material for details). Note that we expect spin noise to make a minor contribution to the linewidth broadening of $cgs \rightarrow\rightarrow 2X_0$ since both the initial and final states cgs and $2X_0$ have a total spin projection of $S = 0$ [43].

IV. FORMATION OF NONLINEAR DRESSED STATES

Finally, we discuss the emergence of new dressed eigenstates of the LA-phonon reservoir coupled four-level system under resonant two-photon excitation $cgs \rightarrow\rightarrow 2X_0$. In the bare-state picture of the system presented in Fig. 3(a), the states cgs, $X_0(H/V)$, and $2X_0$ represent the eigenstates of the system for $\Omega_R = 0$. However, if the system is nonlinearly driven by the excitation laser with a Rabi energy $\Omega_R > 0$, we have to consider two effects: First, the driving field with Rabi energy Ω_R couples $|cgs\rangle$ to $|2X_0\rangle$ to form new nonlinearly dressed eigenstates, illustrated in Fig. 3(a). Second, the excitation field $\hbar\omega_L$ is detuned from the single-photon transitions $cgs \rightarrow X_0(H/V)$ and $X_0(H/V) \rightarrow 2X_0$ by Δ_b. However, for high P_{exc} these states will also be coupled via the ac Stark effect Δ_{AC}. Thus, the Rabi energy Ω_R will admix all four bare states cgs, $X_0(H/V)$, and $2X_0$ into new dressed eigenstates φ_{1-4} presented in Fig. 3(b). Here, we consider the system in a frame rotating with frequency ω_{exc} of the excitation laser. The dominant split in energy between the dressed states $\varphi_{1/3}$ and $\varphi_{2/4}$ is still given by the binding energy $\Delta_b > \Omega_R$. However, the bare-state neutral exciton transitions $X_0(H/V) \rightarrow cgs$ now correspond to transitions between the dressed states $\varphi_{2/4} \rightarrow \varphi_{1/3}$, whose energies are tuned by the Rabi energy

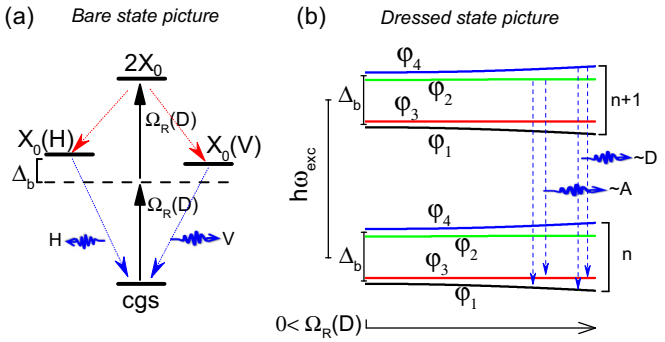

FIG. 3. (a) Bare-state picture of the excitonic system driven on the two-photon resonance $cgs \rightarrow\rightarrow 2X_0$. The D-polarized excitation laser with energy $\hbar\omega_L$ and Rabi energy Ω_R is detuned from the neutral exciton transitions $X_0(H/V)$ by half the binding energy Δ_b. (b) The Rabi energy $\Omega_R(D)$ couples the four bare-state levels cgs, $X_0(H/V)$, and $2X_0$ to form nonlinearly dressed states φ_{1-4}. For a high photon flux of the excitation laser, spontaneous emission occurs between the dressed-state manifolds of $n + 1 \rightarrow n$ photons.

Ω_R. Photons from the system are generated by spontaneous emission between the dressed-state manifolds of $n + 1 \rightarrow n$ photons. Notably, not only is the energy of the states φ_{1-4} tuned by the Rabi energy Ω_R, but so is the polarization of the optical transitions $\varphi_{2/4} \rightarrow \varphi_{1/3}$.

Considering the optical selection rules of the biexcitonic system, the evolution from bare states to dressed states has direct consequences for the polarization of photons from these optical transitions. In the bare-state biexcitonic systems, transitions *from* the neutral exciton $X_0(H/V) \rightarrow cgs$ and *to* the neutral exciton $2X_0 \rightarrow X_0(H/V)$ are addressed by light with a linear polarization H/V, while coherent superpositions of $X_0(H)$ and $X_0(V)$ can be directly addressed by superpositions of the optical polarizations H and V [44]. Accordingly, the polarization of photons from transitions between the admixed dressed states $\varphi_j^{n+1} \rightarrow \varphi_i^n$ (of the manifolds $n + 1$ and n) is *rotated* with respect to the polarization H/V. For example, the dressed state $|\varphi_2\rangle$ evolves with increasing Rabi energy Ω_R from being mostly equal to the bare state $|\varphi_2\rangle \sim |X_0(V)\rangle$ to a coherent superposition of $|\varphi_2\rangle \sim [|X_0(V)\rangle - |X_0(H)\rangle]$. Accordingly, the polarization of the dressed-state transition $\varphi_2 \rightarrow \varphi_1$, where $|\varphi_1\rangle \sim (|cgs\rangle + |2X_0\rangle)$, is rotated from V towards an antidiagonal polarization $A = (H - V)$ by the optical dressing (details are in the Supplemental Material).

In the experiment we operate in the regime illustrated in Fig. 3(a), where for the highest excitation power the ac Stark shift is comparable to the exchange energy $\Delta_{AC} \sim \delta_0$ and the Rabi frequencies do not exceed the binding energy Δ_b. Thus, the fine structure δ_0 and binding energy Δ_b do not prevent the formation of nonlinearly dressed states $|\varphi_{1-4}\rangle = \sum_i \alpha_i^{1-4}|i\rangle$ with $i = cgs, X_0(H), X_0(V), 2X_0$ but lead to unequal, power-dependent admixtures of the different bare-state components α_i of the dressed states φ_{1-4} (see Supplemental Material for details). Thus, by increasing the driving Ω_R of the diagonally D polarized excitation laser, the nonlinearly dressed eigenstates φ_{2-4} evolve from only weakly admixed bare states into a strongly admixed coherent superposition of the different bare eigenstates cgs, $X_0(V)$, $X_0(H)$, and $2X_0$.

To experimentally resolve the nonlinear dressing of the states, we performed high-resolution spectroscopy on the $X_0(V/H) \rightarrow cgs$ transitions using a Fabry-Pérot interferometer with a free spectral range of 124 μeV and a resolution finer than < 1 μeV. Exemplary spectra are presented in Fig. 4(b). For the lowest P_{exc}, we already resolve that each fine-structure peak of the transitions $X_0(V/H) \rightarrow cgs$ is split into two peaks due to the nonlinear dressing of the system. For increasing P_{exc}, the splitting emerging from $X_0(V) \rightarrow cgs$ is increased. At the same time the second set of transitions from $X_0(H) \rightarrow cgs$ is strongly suppressed. These observations are entirely in accord with our expectations and result from a modification of the polarization selection rules of the optical transitions upon dressing. In our experimental setup, we use an $\sim D/A$ cross-polarized excitation/detection scheme to suppress stray light from the excitation laser. Thus, we only resolve the two transitions emerging from $X_0(V) \rightarrow cgs$ in Fig. 4(b) that are polarized predominantly along $\sim A$, while the second set of transitions polarized along $\sim D$ is suppressed (details are in the Supplemental Material).

To obtain quantitative results we numerically calculate the evolution of the dressed-state transitions $\varphi_i^{n+1} \rightarrow \varphi_j^n$ emerging

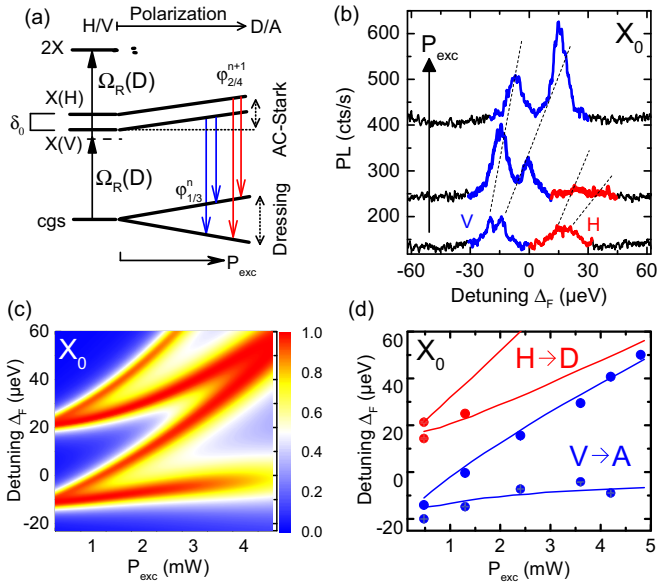

FIG. 4. (a) Schematic evolution of the states cgs, $X_0(H/V)$, and $2X_0$ under resonant two-photon excitation with Rabi energy Ω_R. For Rabi frequencies exceeding the fine structure δ_0, the polarization of the emitted photons is rotated from the polarization basis of the fine-structure H/V into that of the excitation laser D/A. (b) Sample Fabry-Pérot spectra of the $X_0 \rightarrow cgs$ transitions for increasing excitation power P_{exc}. (c) Calculated optical transitions evolving from bare state $X_0(H(V)) \rightarrow cgs$ to dressed state $\varphi_j^{n+1} \rightarrow \varphi_i^n$ transitions as a function of P_{exc}. (d) Peak positions from experiment and theory in (b) and (c), respectively.

from $X_0(H/V) \rightarrow cgs$. Figure 4(c) presents the spectrum from the Hamiltonian $H = H_{QD} + H_{\mathrm{int}} + H_{QD-\mathrm{phonon}}$ that also includes the LA-phonon interaction. The initial transitions between $X_0(V) \rightarrow cgs$ [$X_0(H) \rightarrow cgs$] are split with increasing excitation power and are shifted to higher energies as discussed above. We remark here that the linewidth of the transitions exhibits an additional broadening, while the effective Rabi energy is weakly renormalized due to the charge-carrier-LA-phonon coupling. Finally, we plot in Fig. 4(d) the extracted peak positions from the high-resolution fluorescence spectra in Fig. 4(b) together with the calculated energies of the dressed-state transitions in Fig. 4(c) and observe excellent agreement. Importantly, no further fitting parameters were included after previously adapting the model to the experimentally measured population distributions [Fig. 2(a)]. The evolution of the optical transitions corresponds to the formation of dressed states induced by the nonlinear two-photon excitation of the system, the hallmark of two-photon resonance fluorescence.

V. SUMMARY AND OUTLOOK

In summary, we presented two-photon resonance fluorescence studies on a single QD. We directly mapped out the linewidths of the nonlinear two-photon transitions and determined them to be similar to that of single-photon transitions in the same quantum emitter. Power-dependent measurements revealed the two-photon nature of the absorption process by the observation of an S-shaped saturation behavior of the population evolution in the system. We demonstrated that agreement with an atomic four-level system can only be achieved by including the interaction with LA phonons that lead to a redistribution of the population between the levels. Finally, we demonstrated the formation of nonlinear dressed states and tuning of the polarization selection rules in the system due to the two-photon excitation of the QD and found excellent agreement for *all* features with numerical calculations.

Our results pave the way for investigating a wealth of theoretically predicted optical phenomena resulting from nonlinear resonance fluorescence. They range from fundamental quantum optical effects such as the generation of squeezed light [19,45] or photon bundles with arbitrary quantum statistics [20] to phenomena required for quantum technologies such as the generation of entangled photon pairs from nonlinear dressed states [20]. Considering the superior coherences of photons generated by resonant excitation [7], we anticipate nonlinear resonance fluorescence on QDs embedded in a Purcell enhancing cavity [20] to become a source of entangled photon pairs with unprecedentedly high flux and coherences. Such photon pairs represent ideal candidates for quantum communication protocols [13,46].

Note added. Recently, we became aware of Ref. [47], which reported on similar results.

ACKNOWLEDGMENT

We gratefully acknowledge financial support from the DFG via SFB-631, Nanosystems Initiative Munich, the EU via the ITN S^3 Nano, and BaCaTeC.

[1] H. J. Kimble, M. Dagenais, and L. Mandel, Phys. Rev. Lett. **39**, 691 (1977).
[2] F. Schuda, C. Stroud, Jr., and M. Hercher, J. Phys. B **7**, L198 (1974).
[3] E. Flagg, A. Muller, J. Robertson, S. Founta, D. Deppe, M. Xiao, W. Ma, G. Salamo, and C. Shih, Nat. Phys. **5**, 203 (2009).
[4] A. Vamivakas, Y. Zhao, C. Lu, and M. Atatüre, Nat. Phys. **5**, 198 (2009).
[5] A. Muller, E. B. Flagg, P. Bianucci, X. Y. Wang, D. G. Deppe, W. Ma, J. Zhang, G. J. Salamo, M. Xiao, and C. K. Shih, Phys. Rev. Lett. **99**, 187402 (2007).
[6] X. Xu, B. Sun, P. Berman, D. Steel, A. Bracker, D. Gammon, and L. Sham, Science **317**, 929 (2007).
[7] P. Michler, A. Kiraz, C. Becher, W. Schoenfeld, P. Petroff, L. Zhang, E. Hu, and A. Imamoglu, Science **290**, 2282 (2000).
[8] C. Matthiesen, M. Geller, C. H. Schulte, C. Le Gall, J. Hansom, Z. Li, M. Hugues, E. Clarke, and M. Atatüre, Nat. Commun. **4**, 1600 (2013).
[9] C. Matthiesen, A. N. Vamivakas, and M. Atatüre, Phys. Rev. Lett. **108**, 093602 (2012).
[10] R. Proux, M. Maragkou, E. Baudin, C. Voisin, P. Roussignol, and C. Diederichs, Phys. Rev. Lett. **114**, 067401 (2015).

[11] H. Nguyen, G. Sallen, C. Voisin, P. Roussignol, C. Diederichs, and G. Cassabois, Appl. Phys. Lett. **99**, 261904 (2011).
[12] C. Schulte, J. Hansom, A. Jones, C. Matthiesen, C. Le Gall, and M. Atatüre, Nature (London) **525**, 222 (2015).
[13] J.-W. Pan, Z.-B. Chen, C.-Y. Lu, H. Weinfurter, A. Zeilinger, and M. Żukowski, Rev. Mod. Phys. **84**, 777 (2012).
[14] M. Alexanian and S. K. Bose, Phys. Rev. A **74**, 063418 (2006).
[15] C. Mavroyannis, Opt. Commun. **26**, 453 (1978).
[16] D. A. Holm and M. Sargent, Opt. Lett. **10**, 405 (1985).
[17] B. Sobolewska, Opt. Commun. **20**, 378 (1977).
[18] M. Alexanian and S. K. Bose, Phys. Rev. A **76**, 055401 (2007).
[19] Z. Ficek and R. Tanas, Quantum Opt. **6**, 95 (1994).
[20] C. Sánchez Muñoz, F. P. Laussy, C. Tejedor, and E. del Valle, New J. Phys. **17**, 123021 (2015).
[21] O. Gazzano, S. M. de Vasconcellos, C. Arnold, A. Nowak, E. Galopin, I. Sagnes, L. Lanco, A. Lemaître, and P. Senellart, Nat. Commun. **4**, 1425 (2013).
[22] C. Arnold, J. Demory, V. Loo, A. Lemaître, I. Sagnes, M. Glazov, O. Krebs, P. Voisin, P. Senellart, and L. Lanco, Nat. Commun. **6**, 6236 (2015).
[23] A. Vamivakas, C.-Y. Lu, C. Matthiesen, Y. Zhao, S. Fält, A. Badolato, and M. Atatüre, Nature (London) **467**, 297 (2010).
[24] A. Delteil, W. B. Gao, P. Fallahi, J. Miguel-Sanchez, and A. Imamoğlu, Phys. Rev. Lett. **112**, 116802 (2014).
[25] S. Stufler, P. Machnikowski, P. Ester, M. Bichler, V. M. Axt, T. Kuhn, and A. Zrenner, Phys. Rev. B **73**, 125304 (2006).
[26] H. Jayakumar, A. Predojević, T. Huber, T. Kauten, G. S. Solomon, and G. Weihs, Phys. Rev. Lett. **110**, 135505 (2013).
[27] P. L. Ardelt, L. Hanschke, K. A. Fischer, K. Müller, A. Kleinkauf, M. Koller, A. Bechtold, T. Simmet, J. Wierzbowski, H. Riedl, G. Abstreiter, and J. J. Finley, Phys. Rev. B **90**, 241404 (2014).
[28] S. Bounouar, M. Müller, A. M. Barth, M. Glässl, V. M. Axt, and P. Michler, Phys. Rev. B **91**, 161302 (2015).
[29] M. Müller, S. Bounouar, K. D. Jöns, M. Glässl, and P. Michler, Nat. Photon. **8**, 224 (2014).
[30] J. H. Quilter, A. J. Brash, F. Liu, M. Glässl, A. M. Barth, V. M. Axt, A. J. Ramsay, M. S. Skolnick, and A. M. Fox, Phys. Rev. Lett. **114**, 137401 (2015).
[31] W. Gao, P. Fallahi, E. Togan, J. Miguel-Sánchez, and A. Imamoglu, Nature (London) **491**, 426 (2012).
[32] R. J. Warburton, C. Schäflein, D. Haft, F. Bickel, A. Lorke, K. Karrai, J. M. Garcia, W. Schoenfeld, and P. M. Petroff, Nature (London) **405**, 926 (2000).
[33] R. J. Warburton, B. T. Miller, C. S. Dürr, C. Bödefeld, K. Karrai, J. P. Kotthaus, G. Medeiros-Ribeiro, P. M. Petroff, and S. Huant, Phys. Rev. B **58**, 16221 (1998).
[34] See Supplemental Material at http://link.aps.org/supplemental/10.1103/PhysRevB.93.165305 for measurements of the photonic coherences under resonant two-photon excitation, an analysis of the composition of the new dressed eigenstates of the Hamiltonian $H_{\mathrm{QD}} + H_{\mathrm{int}}$ as well as the polarization of the transitions between them and full details of the numerical calculations presented in the paper.
[35] J. Johansson, P. Nation, and F. Nori, Comput. Phys. Commun. **183**, 1760 (2012).
[36] J. Johansson, P. Nation, and F. Nori, Comput. Phys. Commun. **184**, 1234 (2013).
[37] A. F. Linskens, I. Holleman, N. Dam, and J. Reuss, Phys. Rev. A **54**, 4854 (1996).
[38] S. Weiler, A. Ulhaq, S. M. Ulrich, D. Richter, M. Jetter, P. Michler, C. Roy, and S. Hughes, Phys. Rev. B **86**, 241304 (2012).
[39] M. Glässl, A. M. Barth, and V. M. Axt, Phys. Rev. Lett. **110**, 147401 (2013).
[40] R.-C. Ge, S. Weiler, A. Ulhaq, S. Ulrich, M. Jetter, P. Michler, and S. Hughes, Opt. Lett. **38**, 1691 (2013).
[41] H. S. Nguyen, G. Sallen, C. Voisin, P. Roussignol, C. Diederichs, and G. Cassabois, Phys. Rev. Lett. **108**, 057401 (2012).
[42] J. Houel, A. Kuhlmann, L. Greuter, F. Xue, M. Poggio, B. Gerardot, P. Dalgarno, A. Badolato, P. Petroff, A. Ludwig *et al.*, Phys. Rev. Lett. **108**, 107401 (2012).
[43] A. Kuhlmann, J. Houel, A. Ludwig, L. Greuter, D. Reuter, A. Wieck, M. Poggio, and R. Warburton, Nat. Phys. **9**, 570 (2013).
[44] K. Müller, T. Kaldewey, R. Ripszam, J. S. Wildmann, A. Bechtold, M. Bichler, G. Koblmüller, G. Abstreiter, and J. J. Finley, Sci. Rep. **3**, 1906 (2013).
[45] H. Huang, G. X. Li, W. J. Gu, and Z. Ficek, Phys. Rev. A **90**, 023815 (2014).
[46] A. Aspuru-Guzik and P. Walther, Nat. Phys. **8**, 285 (2012).
[47] F. Hargart, M. Müller, K. Roy-Choudhury, S. L. Portalupi, C. Schneider, S. Höfling, M. Kamp, S. Hughes, and P. Michler, Phys. Rev. B **93**, 115308 (2016).